Numerical Modelling of a Cascadia Subduction Zone Tsunami at the Canadian Coast Guard Base in Victoria, British Columbia

Isaac V. Fine, Richard E. Thomson, Lauren M. Lupton and Stephen Mundschutz

Ocean Sciences Division

Fisheries and Oceans Canada

Institute of Ocean Sciences

9860 West Saanich Road

Sidney, BC

V8L 4B2

2018

Canadian Technical Report of Hydrography and Ocean Sciences 324

Fisheries and Oceans Canada | Pêches et Océans Canada

Canada

Canadian Technical Report of Hydrography and Ocean Sciences

Technical reports contain scientific and technical information of a type that represents a contribution to existing knowledge but which is not normally found in the primary literature. The subject matter is generally related to programs and interests of the Oceans and Science sectors of Fisheries and Oceans Canada.

Technical reports may be cited as full publications. The correct citation appears above the abstract of each report. Each report is abstracted in the data base Aquatic Sciences and Fisheries Abstracts.

Technical reports are produced regionally but are numbered nationally. Requests for individual reports will be filled by the issuing establishment listed on the front cover and title page.

Regional and headquarters establishments of Ocean Science and Surveys ceased publication of their various report series as of December 1981. A complete listing of these publications and the last number issued under each title are published in the Canadian Journal of Fisheries and Aquatic Sciences, Volume 38: Index to Publications 1981. The current series began with Report Number 1 in January 1982.

Rapport technique canadien sur l'hydrographie et les sciences océaniques

Les rapports techniques contiennent des renseignements scientifiques et techniques qui constituent une contribution aux connaissances actuelles mais que l'on ne trouve pas normalement dans les revues scientifiques. Le sujet est généralement rattaché aux programmes et intérêts des secteurs des Océans et des Sciences de Pêches et Océans Canada.

Les rapports techniques peuvent être cités comme des publications à part entière. Le titre exact figure au-dessus du résumé de chaque rapport. Les rapports techniques sont résumés dans la base de données Résumés des sciences aquatiques et halieutiques.

Les rapports techniques sont produits à l'échelon régional, mais numérotés à l'échelon national. Les demandes de rapports seront satisfaites par l'établissement auteur dont le nom figure sur la couverture et la page de titre.

Les établissements de l'ancien secteur des Sciences et Levés océaniques dans les régions et à l'administration centrale ont cessé de publier leurs diverses séries de rapports en décembre 1981. Vous trouverez dans l'index des publications du volume 38 du Journal canadien des sciences halieutiques et aquatiques, la liste de ces publications ainsi que le dernier numéro paru dans chaque catégorie. La nouvelle série a commencé avec la publication du rapport numéro 1 en janvier 1982.

Canadian Technical Report of
Hydrography and Ocean Sciences 324

2018

NUMERICAL MODELLING OF A CASCADIA SUBDUCTION ZONE TSUNAMI AT THE CANADIAN COAST GUARD BASE IN VICTORIA, BRITISH COLUMBIA

by

Isaac V. Fine, Richard E. Thomson, Lauren M. Lupton and Stephen Mundschutz

Ocean Sciences Division
Fisheries and Oceans Canada
Institute of Ocean Sciences
9860 West Saanich Road
Sidney, BC, V8L

© Her Majesty the Queen in Right of Canada, 2018.

Cat. No. Fs97-18/324E-PDF ISBN 978-0-660-25299-5 ISSN 1488-5417

Correct citation for this publication:

Isaac V. Fine, Richard E. Thomson, Lauren M. Lupton and Stephen Mundschutz 2018. Numerical Modelling of a Cascadia Subduction Zone Tsunami at the Canadian Coast Guard Base in Victoria, British Columbia. Can. Tech. Rep. Hydrogr. Ocean Sci. 324: v + 30p.

CONTENTS

1 CASCADIA SUBDUCTION ZONE EARTHQUAKES AND TSUNAMI 1

2 NUMERICAL SIMULATION OF A CASCADIA SUBDUCTION ZONE TSUNAMI 3

2.1 Model Setup: Nested Grid Formulation 3

2.1.1 Coarse Grid (Grid 1) 4

2.1.2 Intermediate Grid (Grid 2) 5

2.1.3 Intermediate Grid (Grid 3) 7

2.1.4 Final Grid (Grid 4) 8

2.2 Model Reference Level 9

2.3 Tsunami Source Distributions 9

3 RESULTS 11

3.1 Comparison of Modelled Tsunami Waves for Two Cascadia Subduction Zone Scenarios for Coarse and Intermediate Grids 11

3.2 Detailed Results for Victoria Harbour Canadian Coast Guard Base: Variations in Sea Level and Tsunami-Induced Currents 13

4 CONCLUSIONS 25

5 ACKNOWLEDGEMENTS 27

6 REFERENCES 29

ABSTRACT

Numerical Modelling of a Cascadia Subduction Zone Tsunami at the Canadian Coast Guard Base in Victoria, British Columbia

Isaac V. Fine, Richard E. Thomson, Lauren M. Lupton and Stephen Mundschutz, 2018. Numerical Modelling of a Cascadia Subduction Zone Tsunami at the Canadian Coast Guard Base in Seal Cove, Prince Rupert, British Columbia. Tech. Rep. Hydrogr. Ocean Sci. 324: v + 30p.

The last major megathrust earthquake along the Cascadia Subduction Zone (CSZ) off the west coast of North America occurred in January 1700. The massive tsunami waves generated by this moment magnitude (Mw) 9.0 event caused significant destruction as far away as Japan on the opposite side of the Pacific Ocean. Future CSZ events pose a high risk for destructive tsunamis for the British Columbia coast.

This work uses a nested-grid numerical tsunami model to predict the tsunami waves and currents at Victoria generated by a Mw 9.0 CSZ failure. Two updated earthquake source models are used: A buried rupture model (A) and a splay-fracture model (B). Both models include new source areas to the west of Vancouver Island. The analysis is in anticipation of upgrades and modernization of the Canadian Coast Guard base at Victoria.

Tsunami wave amplitudes at Victoria estimated by the splay-fracture Model B are highest, reaching 2.26 m above the tidal level, compared to 1.72 m by Model A. The first wave is the highest, arriving 1.5 hours after the start of the earthquake. The subsidence of 0.2 m that follows a CSZ earthquake will increase the total height of the tsunami wave to 2.46 above the tidal level or 3.19 m above Mean Sea Level. Wave induced currents at the base will be weak but reach speeds of around 1.76 m/s around Shoal Point. Incorporation of a 50% safety factor gives a safe water level for Victoria of 4.79 m above Mean Sea Level for a Model B type event.

RESUME

Modélisation numérique d'un tsunami à proximité de la zone de subduction de Cascadia à la base de la Garde côtière canadienne de Victoria, Colombie-Britannique

Isaac V. Fine, Richard E. Thomson, Lauren M. Lupton and Stephen Mundschutz, 2018. Numerical Modelling of a Cascadia Subduction Zone Tsunami at the Canadian Coast Guard Base in Seal Cove, Prince Rupert, British Columbia. Tech. Rep. Hydrogr. Ocean Sci. 324: v + 30p.

Le dernier mégaséisme majeur le long de la zone de subduction de Cascadia (ZSC) au large de la côte ouest de l'Amérique du Nord est survenu en janvier 1700. Les vagues sismiques

océaniques générées par ce séisme de 9,0 sur l'échelle de magnitude de moment (Mw) ont causé des dégâts considérables aussi loin que le Japon, de l'autre côté de l'océan Pacifique. L'activité sismique potentielle future le long de la ZSC pourrait engendrer des tsunamis destructeurs posant des risques importants pour la côte de la Colombie-Britannique.

Ce projet utilise un modèle de tsunami numérique à grille à maille variable afin de prédire les vagues sismiques océaniques et les courants à Victoria en cas de séisme de 9,0 Mw le long de la ZSC. Deux modèles de source des séismes sont utilisés : le modèle de rupture enfouie (A) et le modèle de fracture de la faille subsidiaire d'amortissement (B). Les deux modèles comprennent de nouvelles zones sources à l'ouest de l'île de Vancouver. L'analyse est effectuée dans le cadre des initiatives futures de mise à niveau et de modernisation de l'installation de la Garde côtière à Victoria.

L'amplitude des vagues sismiques océaniques à Victoria estimée à partir du modèle de fracture de la faille subsidiaire d'amortissement, B, est plus élevée, atteignant 2,26 m au-dessus du niveau de marée, par rapport à 1,72 m pour le modèle A. La première vague serait la plus haute, arrivant 1,5 h après le début du séisme. La subsidence de 0,2 m suivant un séisme le long de la ZSC ferait augmenter la hauteur totale de la vague sismique océanique à 2,46 m au-dessus du niveau de marée, soit 3,19 m au-dessus du niveau moyen de la mer. Les courants engendrés par les vagues à la base ne seraient pas très puissants, mais atteindraient des vitesses d'environ 1,76 m/s dans les environs de Shoal Point. L'intégration d'un facteur de sécurité de 50 % permet d'obtenir un niveau d'eau sécuritaire pour Victoria de 4,79 m au-dessus du niveau moyen de la mer pour un événement du type décrit par le modèle B.

Photo of Victoria Harbour by Dan Blanchard, made on September 17,2017

1 CASCADIA SUBDUCTION ZONE EARTHQUAKES AND TSUNAMI

Cascadia Subduction Zone (CSZ) tsunamis are the main tsunami threat for the west coast of British Columbia (Clague et al., 2003; Leonard et al., 2014). The Great CSZ earthquake of 26 January 1700 (moment magnitude, Mw = 9.0) generated a major trans-oceanic tsunami that caused significant destruction in Japan and strongly affected the west coasts of the USA and Canada. Results from recent paleotsunami studies along the coast of Vancouver Island and the west coast of the USA (cf. Clague, 2000), show evidence of the event and the associated extent of the intense flooding along the California, Oregon, Washington and Vancouver Island coasts (Atwater et al., 1995; Satake et al., 1996). Following these studies investigations of CSZ tsunamis dramatically increased.

Preliminary numerical modelling of CSZ tsunamis for coastal North America (cf. Chemiawsky et al., 2007; Fine et al., 2008; Cheung et al., 2011, AECOM, 2013), demonstrate the high risk of CSZ tsunamis for British Columbia. Numerous seismotectonic studies indicate that great megathrust earthquakes in the CSZ region have occurred on a regular basis in the past and can be expected to occur with an average return period of about 500 years in the foreseeable future (Witter et al., 2013; Wang and Tréhu, 2016).

The 1100 km long CSZ extends from Cape Mendocino in northern California to central Vancouver Island (Figure 2.1). Subduction of the Pacific Plate beneath the North American Plate takes place about 100 km to the west of Vancouver Island. Given the relatively long seismic quiescence, this region is now considered under high risk from a major megathrust earthquake and consequent tsunami that could strike the southwest coast of British Columbia (Dragert and Rogers, 1988). As part of natural hazard risk mitigation studies, several investigators have undertaken numerical computations of potential tsunamis originating from a megathrust CSZ failure along the North America coast (e.g., Ng et al., 1990, 1991; Whitmore, 1993).

The purpose of this report is to present results of numerically simulated tsunami waves that could be generated by a CSZ earthquakes of Mw = 9.0. Focus is on estimating the magnitude and arrival times for the expected tsunami waves for the Canadian Coast Guard Base at Victoria, British Columbia. This research is part of a larger study to inform future redesigns of Canadian Coast Guard stations around the British Columbia coastline, to mitigate the impact on the operability at these stations in the event of a major earthquake generated tsunami.

Initial studies showed that tsunamis generated by a Mw ~9.0 CSZ earthquake could present a major threat to the west coast of the United States and southwest coast of British Columbia. The estimated wave runup for the January 1700 Cascadia tsunami along the west coastlines of North America was up to 20 m (Atwater et al., 1995). Further numerical studies were undertaken to estimate possible tsunami risk for settlements along the outer, west coast of Vancouver Island associated with such earthquakes (cf. Myers et al., 1999; Cherniawsky et al., 2007; Fine et al., 2008; Cheung et al., 2011). These studies used source models that reflected the current science at the time of the respective study. Detailed characterisation of megathrust rupture models used for simulating tsunami inundation was presented by Witter et al., (2013). The authors examined 15 megathrust earthquake scenarios, looking in detail at three main scenarios.

The splay-fault rupture referred to as Model 1 (M1) is of particular interest for the present study as it best represents a CSZ earthquake given present understanding of the faulting processes. For this model, Witter et al. (2013) used an extremely dense numerical mesh to allow accurate modelling of the surface-breaching rupture. Their model has the following parameters: Length = 1000 km; width = 83 km; maximum slip = 18 m; average slip = 9 m; seismic moment = 2.9·1022 N·m; and Mw = 8.9. This work uses a slightly modified version of the model according to the recommendations of Wang and Tréhu (2016) to simulate the tsunami risk for Victoria.

2 NUMERICAL SIMULATION OF A CASCADIA SUBDUCTION ZONE TSUNAMI

2.1 MODEL SETUP: NESTED GRID FORMULATION

Accurate numerical simulation of tsunami waves in the rapidly shoaling regions of the west coast of British Columbia requires setting up a model domain as a series of nested grids of ever finer spatial and temporal resolution. The use of nested grids of smaller cell dimensions and time steps makes it possible to resolve tsunami wave configurations as they propagate into the shallow coastal regions. The principal requirements for numerical models using nested grids are as follows:

- Nested grid cell sizes are generally obtained by dividing the initial, large-scale coarse numerical grid by an integer, typically 3 to 5. Integers larger than this can lead to grid interface problems;
- Nested grids are needed in near-coastal areas; the coarse "parent" grid should be of sufficient extent to resolve possible feed-back effects that the nested grid may have on the parent grid during the simulation time;
- A good interface between the inner and outer domains is required to avoid errors and model instability associated with point matching between the different grids. This should allow two-way fluxes without trapping shorter waves at the inner domain boundaries;
- High resolution bathymetry, external forcing and observations are needed for model domain setup, initialization and validation at each domain level; here the nested-grid formulation is similar to that used in well-known tsunami models, TUNAMI and COMCOT (Liu *et al.*, 1998; Imamura, *et al.*, 2006; Wang, 2009).

Dispersion effects can be included in the model by substituting numerical dispersion for the actual physical dispersion. Solving this issue (see for example, Imamura et al., 1988) has made it possible for investigators to cover large, open ocean regions, representative of an area affected by a CSZ tsunami, using a relatively coarse grid with a cell size of roughly 10 km by 10 km (4-5 arc-seconds).

Because of the relatively long periods of the tsunamis generated in the deep-water source regions used in this study, and because of the relatively short propagation times of 1 to 2 hours from the source region to the Victoria site, the dispersion effect is negligible. In this case, high bathymetric resolution is the important factor for modelling wave propagation in the offshore regions.

The present project uses a series of four nested grids for the CSZ tsunami model (Table 1). The choice of model grids takes into account the need for high spatial resolution to accurately resolve the reflection and transformation of the waves and the need for large spatial extent to capture the effects of frequency dispersion during long distance wave propagation.

Table 1. Parameters of the numerical grids used in the tsunami generation and propagation model. Grid extent is along the x (eastward) and y (northward) coordinate directions and is presented in degrees (°). Numerical grid cell sizes for Grids 2, 3 and 4 are roughly 270, 54 and 11 m, respectively. Columns 2, 3 and 4 are presented as x, y values. CHS refers to the Canadian Hydrographic Service.

Grid No.	Extent (x, y) (degrees)	Array (number of grid points)	Cell size (degrees)	Source of data	Processing type
1	18.0, 17.0	720,1361	0.025, 0.0125	GEBCO 2014 30 arc- seconds gridded data	Filtering and bilinear interpolation
2	2.45, 1.95	589,780	0.00416667, 0.0025	BC 3 arc-sec bathymetric DEM	Filtering and bilinear interpolation
3	0.252, 0.21	291, 505	0.0008333, 0.0004167	BC 3 arc-sec bathymetric DEM	Filtering and bilinear interpolation
4	0.123, 0.0766	740, 920	0.000166667, 0.0000833	CHS bathymetry data	Kriging, smoothing, bilinear interpolation

2.1.1 Coarse Grid (Grid 1)

Grid 1 is the coarsest numerical grid used in the model. This large-scale grid covers the northeast Pacific and encompasses the major source region used in the simulations for the CSZ. The northeast Pacific is an important tsunami wave generation region through which all offshore tsunamis propagate on their way to coastal British Columbia. The grid was created using the 30 arc-second global bathymetry dataset GEBCO 2014 (Becker et al., 2009).

The spatial resolution of the coarse grid is 90 arc-seconds in the east-west (x) direction (spatial scales ranging from 1.4 km to 2.2 km, depending on latitude) and 45 arc-seconds in the north-south (y) direction (1.4 km grid size). The grid spans the northeast Pacific and is bounded by 38– 55° N, 140 – 122° W. A typical spatial scale for each grid cell is thus about 1.5 km.

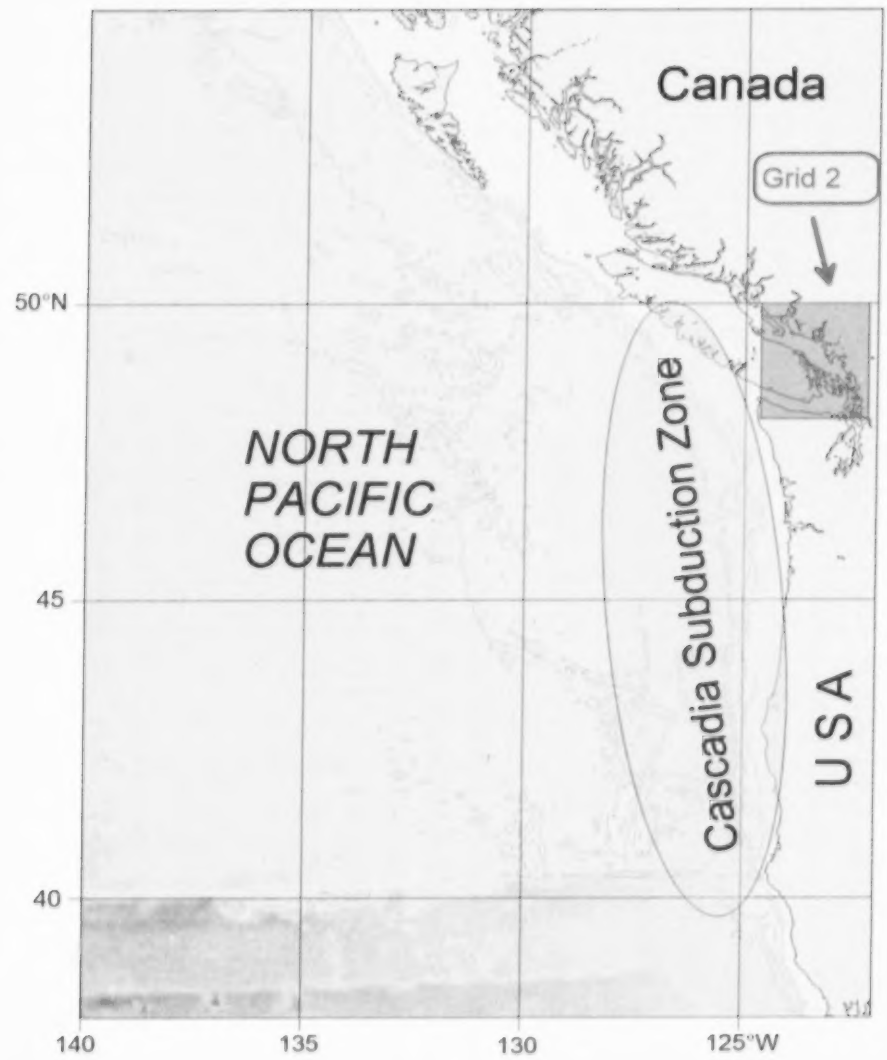

Figure 2.1. The region covered by the large-scale coarse grid numerical model for the northeast Pacific (Grid 1). Also shown is the CSZ where a tsunami could be generated that would impact the Victoria Coast Guard Base. The insert shows the location of the first nested grid (Grid 2), covering the southwest coast of British Columbia.

2.1.2 Intermediate Grid (Grid 2)

Grid 2 covers southern British Columbia and the northwest US coast (Figure 2.2). The location and coverage of the grid was chosen so that it extends equally to the west and to the east of the Victoria region, also covering the shelf region. This intermediate grid is important for simulating wave transformation as the tsunami enters the Salish Sea through Juan de Fuca Strait. This grid is also

important for tsunamis penetrating into the Strait of Georgia through the narrow straits, capturing the energy exchange between the deeper shelf waters and the much shallower coastal zone.

The grid was created using the British Columbia 3 arc-second bathymetric Digital Elevation Model (DEM), (NOAA, 2017). Grid 2 has a resolution of 15 arc-seconds in the east-west direction and 9 arc-seconds in the north-south direction, corresponding to spatial scales (x, y) of approximately 270 m and 280 m, respectively (Table 1). The grid boundaries span 48.2° – 50°N, 124.5° – 122°W.

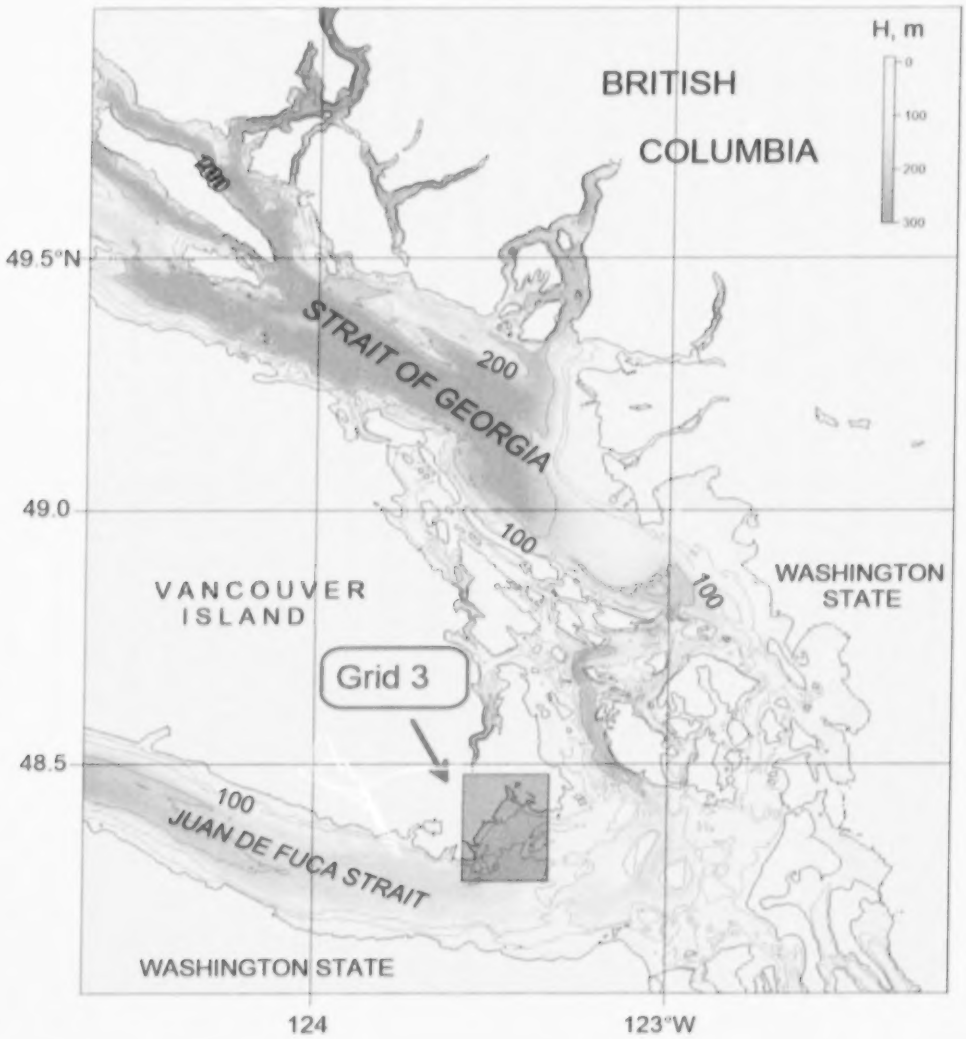

Figure 2.2. The Salish Sea region covered by the medium-scale bathymetric grid (Grid 2) for the southwest coast of British Columbia. The horizontal grid cell scales (x, y) for this region are approximately 270 m by 280 m, respectively. The insert shows the boundaries and location of the second nested grid (Grid 3) covering the region of Victoria. Depths, H, are in metres (m).

2.1.3 Intermediate Grid (Grid 3)

The third numerical grid covers the southern end of Vancouver Island near Victoria and surrounding passes and inlets of Juan de Fuca Strait (Figure 2.3). This grid is of considerable importance since it determines wave transformation in the vicinity of Victoria. Model grid cells were created using the British Columbia 3 arc-second bathymetric DEM (2017). The gridded data were subsequently re-interpolated to a geographical coordinate system (NAD83 standard) with a rectangular grid cell size of 3 arc-seconds by 1.5 arc-seconds (approximately 61 m by 46 m) in the east-west and north-south directions, respectively.

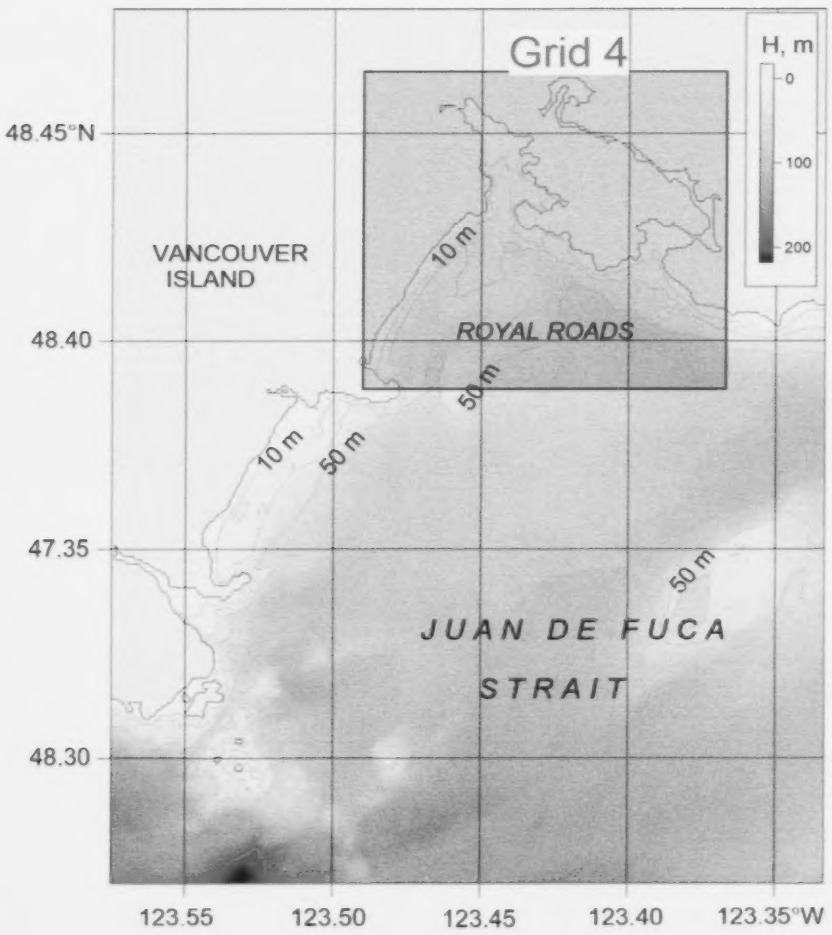

Figure 2.3. The coastal region covered by Grid 3, southern Vancouver Island coast and adjoining Juan de Fuca Strait. The x, y grid scale for this region is approximately 61 m and 46 m, respectively. The insert shows the boundaries and location of the fourth nested grid (Grid 4) covering Esquimalt Harbour and Victoria Harbour. Depths, H, are in metres (m).

2.1.4 Final Grid (Grid 4)

The final (fourth) numerical grid has the highest spatial resolution and covers coastal areas in Victoria (Figure 2.4). The grid has been created for both the Victoria and Esquimalt harbour areas and is designed specifically for estimation of tsunami inundation and tsunami-induced currents in the vicinity of the Coast Guard Base. A Kriging algorithm (Matheron, 1963) was used to create the grid from the original, irregularly-spaced bathymetric data. Details on Kriging can be found in Thomson and Emery (2014).

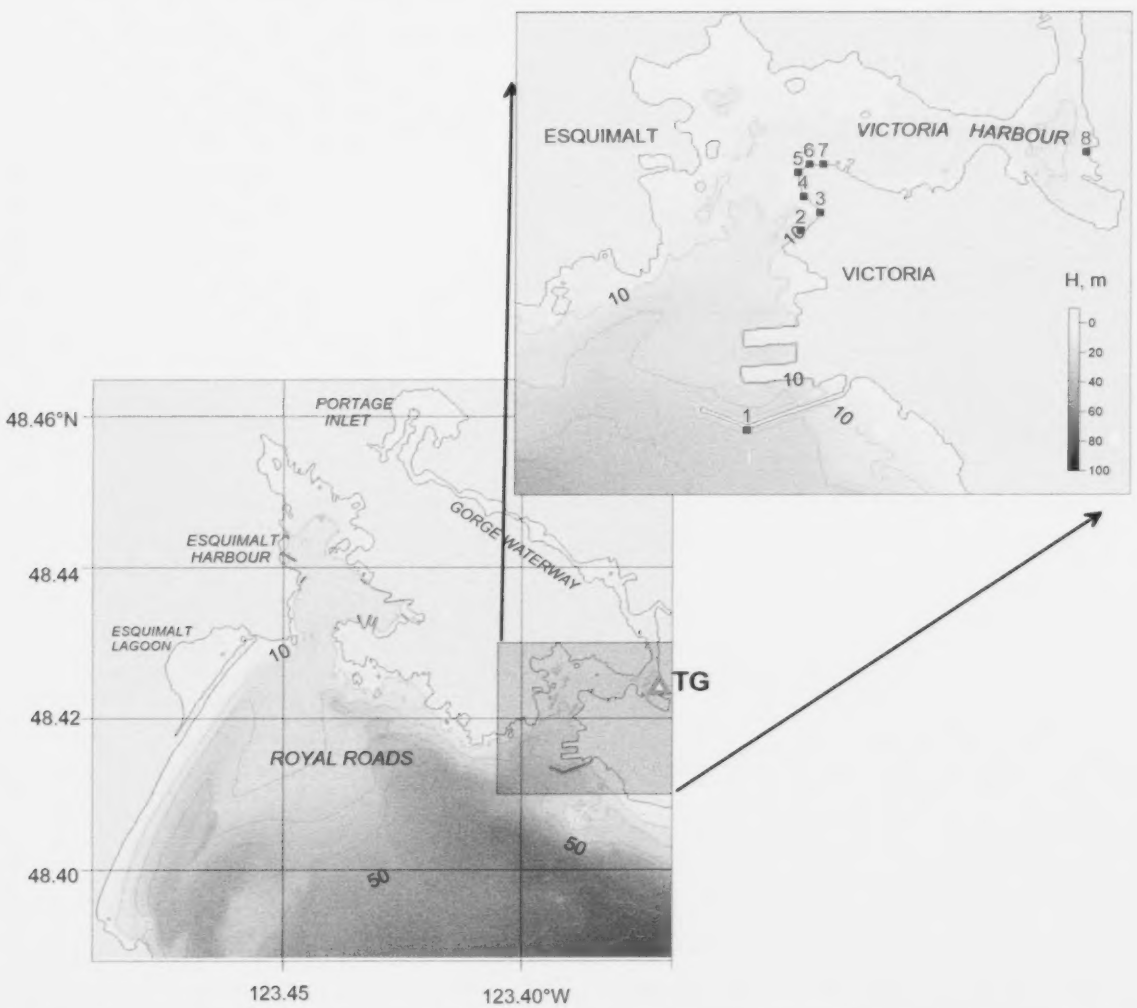

Figure 2.4. The region covered by Grid 4. The fine-scale bathymetric grid has adjusted topography for the region of Victoria Harbour, and has a grid scale (x, y) of approximately 12 m by 9 m, respectively. Also shown are the location of the tide gauge (TG) and the sites (1-8) at Victoria for which tsunami wave records have been simulated. Depths, H, are in metres (m).

2.2 MODEL REFERENCE LEVEL

Model simulations are generally conducted for tsunami arrival times that coincide with times of Mean Higher High Water (MHHW), as per recommendations for computation of tsunami inundation in the United States (National Tsunami Hazard Mapping Program, 2010; Nikolsky et al., 2013). Accordingly, maps of maximum tsunami wave height and current speed in this report are referenced to MHHW rather than to the mean tide or to a geodetic reference.

MHHW is used as a reference level for all modelling results. For the Victoria tide gauge site, MHHW is 0.73 m above Mean Sea Level (MSL). For convenience, a common reference value of 0.73 m is added throughout the region for the tsunami modelling.

However, when examining the waves themselves, the wave height, h, presented in the figures can be considered as the wave crest height measured relative to the tide level at the time of the tsunami arrival. This is a positive value. Sometimes, we want to show the depth of the wave trough, in which case "height" will be negative value measured downward from the tide level at the time of the tsunami.

Table 2. Chart datum values for station 7120 provided by the Canadian Hydrographic Service. Latitude and longitude are in degrees and minutes. Higher High Water (HHW) is defined in two ways: using all tidal values (Mean) and using only the highest tides (Large). Z_0 is the mean tidal constituent obtained by harmonic analysis of the tidal series.

Tide gauge ID	Name	Latitude (°N)		Longitude (°W)		MSL (m)	HHW (m)		Extreme high water (m)
		Deg	Min	Deg	Min	Z_0	Mean	Large	
7120	**Victoria**	48	25.48	123	22.42	1.88	2.61	3.12	3.76

2.3 TSUNAMI SOURCE DISTRIBUTIONS

Based on recent advances in Cascadia tsunami source development (cf. Wang and Tréhu, 2016), we considered two different CSZ earthquake source models for tsunamis impacting the coast of British Columbia: Model A, the "buried" model; and Model B, the "splay" model. The models correspond to the same seismic momentum magnitude (Mw = 9.0) but to different cross-shore distributions of the associated seismic seafloor uplifts, h_0. The models have the northward extensions from the Witter et al. (2013) seismic sources off California to Washington, but also include source areas located to the west of Vancouver Island.

The splay-faulting rupture model includes a contribution of coseismic horizontal displacements to the initial tsunami wave field through a component of ocean surface uplift due to the horizontal motion of the steep ocean bottom slopes (Gao, 2016). Numerical tsunami simulations reveal that including the deformation due to horizontal displacements in the source function, results in an increase in the far-field tsunami amplitudes. The resulting coseismic vertical deformations (h_0) are shown in Figure 2.5.

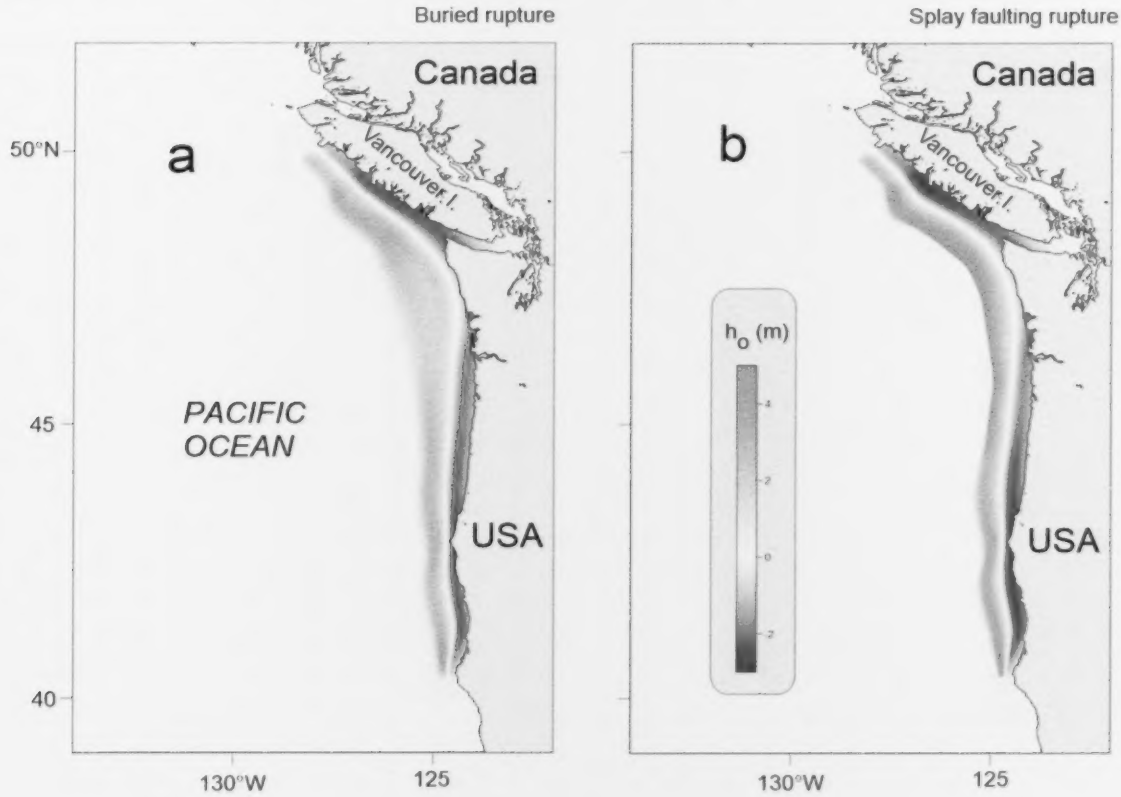

Figure 2.5. Maps of the Cascadia rupture zone tsunami sources according to Gao (2016). Seafloor displacements, h_0, are in metres. (a) Whole margin buried rupture (Model A); and (b) Whole margin splay-faulting rupture (Model B).

Model A is the case when the source deformation slip is located well below the sea bed, whereby the seafloor uplift has a smooth and gentle cross-shore profile, with maximum uplift of 4 m. Model B corresponds to the "splay" model, where the rupture edges are at the sea floor. This model corresponds to the case "M1" in the Witter et al. [2013] classification and can be considered the most probable scenario. Maximum uplift is near 8 m. We note that the two previous models for Cascadia tsunami sources for the British Columbia coast, Cherniawsky et al. [2007] and AECOM [2013], used tsunami sources that are somewhere between Models A and B.

3 RESULTS

3.1 COMPARISON OF MODELLED TSUNAMI WAVES FOR TWO CASCADIA SUBDUCTION ZONE SCENARIOS FOR COARSE AND INTERMEDIATE GRIDS

Low-resolution results for CSZ tsunami simulations for Model A and Model B are presented in Figure 3.1. As these models indicate, maps of the tsunami height maxima (wave crest maxima) for the open ocean are quite different: Model B provides much more intensive waves, with stronger interference of waves arriving from the northern and southern sectors of the CSZ. Waves generated by the splay faulting rupture (Model B) have a stronger impact on coastal areas of Vancouver Island and the US west coast than waves generated by the buried rupture (Model A).

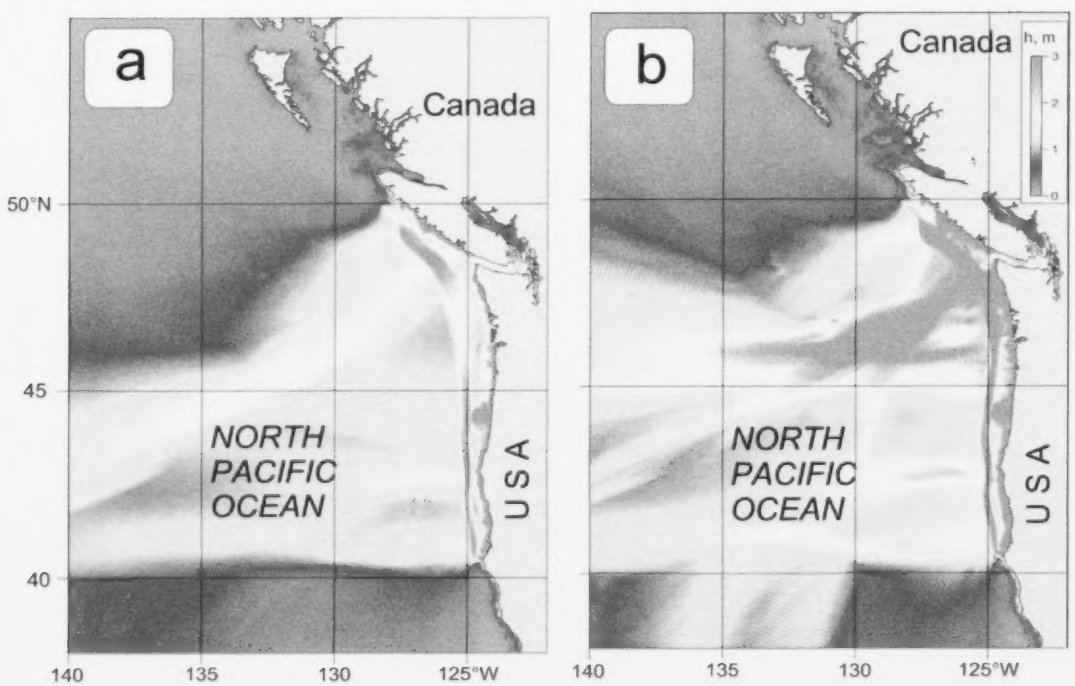

Figure 3.1. Spatial distribution of maximum tsunami wave heights (h, in metres) for Grid 1 of the nested-grid model for waves generated by simulation of the CSZ tsunami for (a) Model A; and (b) Model B.

For southern Vancouver Island (Grid 2, Figure 3.2), the differences between the results for models A and B do not follow a simple pattern. In general, Model B estimates higher wave heights than Model A at the entrance and central part of Juan de Fuca Strait. At the eastern end of Juan de Fuca Strait

and throughout the Strait of Georgia, the heights of the tsunami waves for Model A and Model B are similar. However, around Victoria and Esquimalt harbours, Model B simulates slightly larger tsunami waves.

Figure 3.3 shows the higher resolution Model A and B results for Grid 3, which covers the approach to Victoria and both Victoria and Esquimalt harbours. The resultant tsunami waves are approximately 15 to 20% higher for Model B than for Model A throughout the approach in the Juan de Fuca Strait. The tsunami waves for both models are amplified slightly toward the southern (US) coast. The simulations also show amplification of the tsunami waves in both the harbours, especially in Esquimalt Harbour for both Model A and Model B.

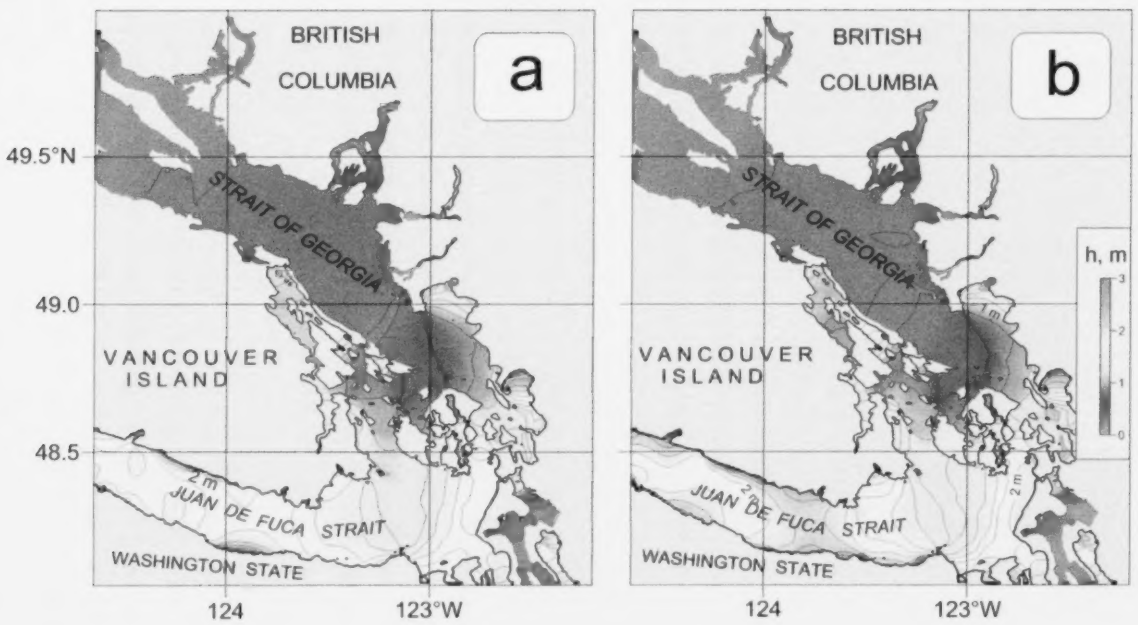

Figure 3.2. Spatial distribution of maximum tsunami wave heights (h, in metres) for Grid 2 of the nested-grid model for waves generated by simulation of the CSZ tsunami for (a) Model A; and (b) Model B.

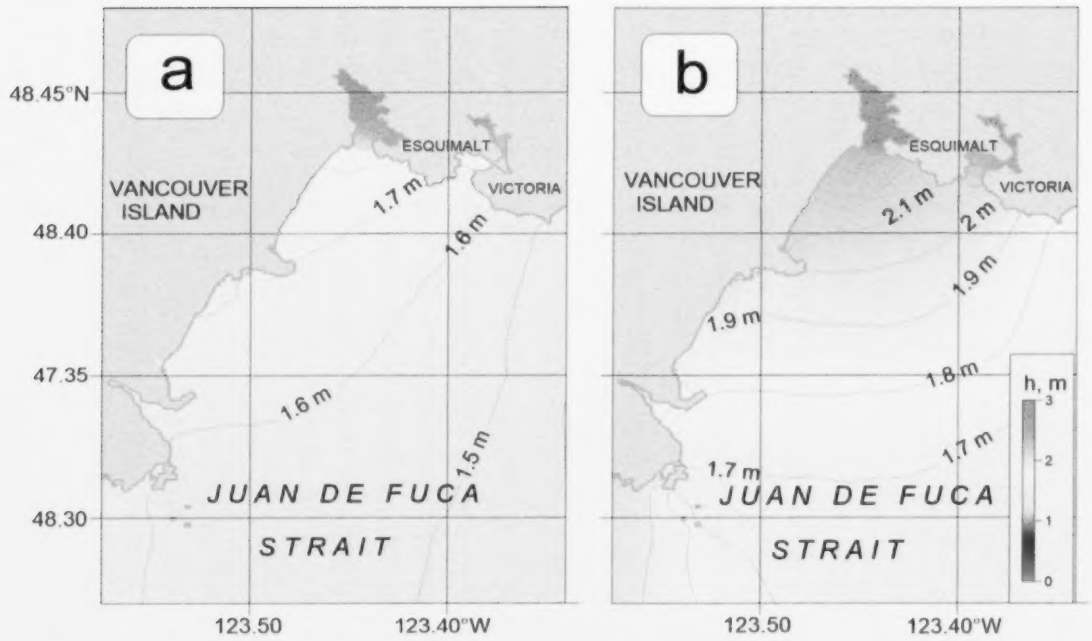

Figure 3.3. Spatial distribution of maximum tsunami wave heights (h, in metres) for Grid 3 of the nested-grid model for waves generated by simulation of the CSZ tsunami for (a) Model A and (b) Model B.

3.2 DETAILED RESULTS FOR VICTORIA HARBOUR CANADIAN COAST GUARD BASE: VARIATIONS IN SEA LEVEL AND TSUNAMI-INDUCED CURRENTS

Detailed distributions of the maximum wave heights and wave-induced currents in Victoria Inner and Outer Harbours and surrounding areas are presented in Figures 3.4-3.5. According to Figure 3.4a, the average maximum tsunami height in Victoria Outer Harbour is about 1.7 m for Model A, and about 2.2 m for Model B. The spatial height distributions are quite similar for both cases, but wave heights for Model B are 30% higher than those for Model A. In Victoria's Inner Harbour, tsunami heights are nearly uniform and gently increase toward the harbour head and in the Gorge Waterway.

The tsunami-induced currents are strong in Victoria Harbour for both cases (Figures 3.5a and 3.5b), especially in the centre of the harbour and around the headlands. As with wave height, currents are stronger for Model B, while the spatial distribution of the currents for both models is again similar.

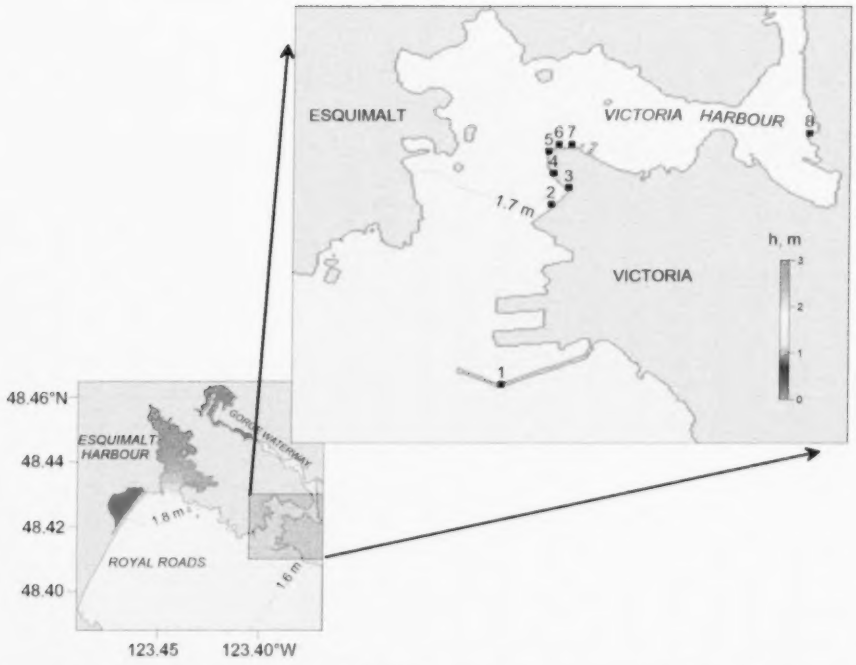

Figure 3.4a. Model A, Grid 4: Distribution of maximum CSZ tsunami wave heights (h, m). The insert shows Victoria Harbour.

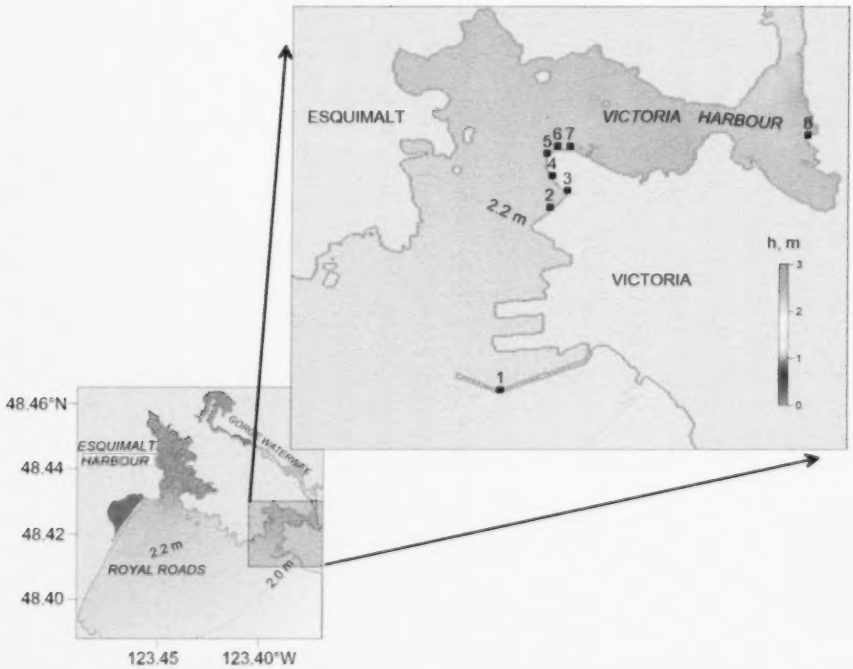

Figure 3.4b. Model B, Grid 4: Distribution of maximum CSZ tsunami wave heights (h, m). The insert shows Victoria Harbour.

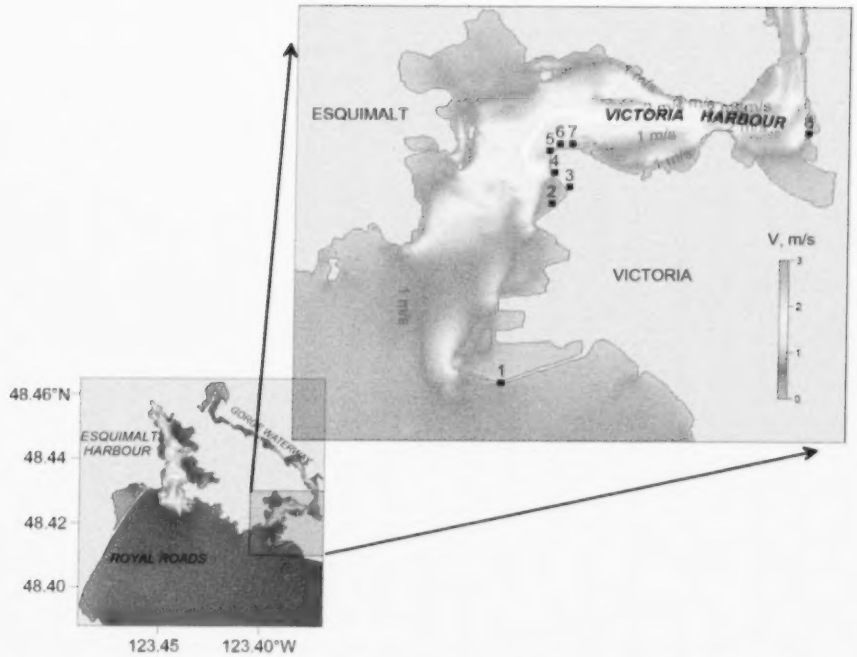
ESQUIMALT
VICTORIA HARBOUR
VICTORIA
V, m/s
1 m/s
1 m/s
1

Time series for Models A and B for the simulated waves and wave-induced currents at specific sites are presented in Figures 3.6 to 3.11; the statistical characteristics are in Tables 3.1, 3.2 and 3.3. For each individual model run, the simulated wave heights for Sites 2 to 7, located at the Canadian Coast Guard Base, are nearly identical, but differ notably from Sites 1 and 8. For both models, the wave heights are lower for Site 1 on the outer side of the water breaker and higher at Site 8, the tide gauge location.

Table 3.1. Tsunami wave parameters for a CSZ tsunami in Victoria Harbour for Model A numerical simulations. See Figure 3.5 for the site locations. Travel times for the maximum waves are in hours and minutes (HH:MM) after the start of the earthquake.

Site No	First trough		Highest crest		Deepest trough	
	Height (m)	Travel time HH:MM	Height (m)	Travel time HH:MM	Height (m)	Travel time HH:MM
1	-0.96	00:52	1.63	01:28	-1.04	02:58
2	-1.00	00:54	1.70	01:29	-1.16	02:56
3	-1.01	00:54	1.71	01:29	-1.16	02:56
4	-1.01	00:54	1.72	01:30	-1.17	02:56
5	-1.02	00:54	1.72	01:30	-1.19	02:57
6	-1.03	00:55	1.72	01:30	-1.22	02:57
7	-1.04	00:55	1.72	01:30	-1.22	02:57
8	-1.09	00:57	1.76	01:32	-1.33	03:00

Table 3.2. Tsunami wave parameters for a CSZ tsunami in Victoria Harbour for the Model B numerical simulations. See Figure 3.5 for the site locations. Travel times for the maximum waves are in hours and minutes (HH:MM) after the start of the earthquake.

Site No	First trough		Highest crest		Deepest trough	
	Height (m)	Travel time HH:MM	Height (m)	Travel time HH:MM	Height (m)	Travel time HH:MM
1	-0.92	00:52	2.02	01:23	-1.24	03:01
2	-0.96	00:54	2.21	01:24	-1.38	03:03
3	-0.96	00:54	2.22	01:24	-1.38	03:03
4	-0.96	00:54	2.23	01:24	-1.38	03:03
5	-0.98	00:54	2.25	01:25	-1.38	03:03
6	-0.99	00:54	2.26	01:25	-1.38	03:04
7	-0.99	00:55	2.26	01:25	-1.23	03:04
8	-1.05	00:57	2.30	01:26	-1.49	03:08

Table 3.3. Wave-induced current speeds (V) for a CSZ tsunami in Victoria Harbour for Models A and B numerical simulations. See Figure 3.5 for the site locations. Travel times for the occurrence of maximum wave-induced currents are in hours and minutes (HH:MM) after the start of the earthquake.

Site No	Model A		Model B	
	Maximum current speed (m/s)	Time of maximum current speed HH:MM	Maximum current speed (m/s)	Time of maximum current speed HH:MM
1	0.47	02:11	0.68	02:09
2	0.28	02:25	0.37	02:23
3	0.01	02:27	0.01	02:12
4	0.29	02:14	0.32	02:09
5	1.41	03:15	1.74	02:13
6	1.35	01:40	1.60	01:32
7	1.07	02:17	1.04	02:33
8	0.76	02:22	1.12	02:22

The earthquake will cause the land in the Victoria area to fall 20 cm immediately after the initial shock. As the leading wave of the incoming tsunami will be a wave trough, sea level in the region will also fall an additional 1 m upon arrival of the first wave roughly 54 minutes after the earthquake for both Model A and B scenarios. After the initial drop caused by the leading wave, the sea level rises in the next half hour. At the Coast Guard Base location (covered by Sites 2 to 7), the highest wave crests predicted are 1.72 m and 2.26 m at 1 hour 30 minutes and 1 hour 25 minutes for Models A and B, respectively.

The second wave crest is only slightly lower than the first crest wave for both cases; the third and subsequent waves are much lower than the first two waves. Typical tsunami wave periods are about 1 hour for both earthquake models.

Wave-induced currents for Site 1 are notably larger than at Sites 2 to 4, reaching almost 0.7 m/s in Model B, whilst the currents around the base range from 0.29 m/s to 0.37 m/s for Models A and B respectively. At Sites 5 to 7 the currents are around 60 % stronger as they propagate around Shoal Point. The strongest currents occur at Site 5 (1.41 m/s for Model A and 1.74 m/s for Model B) located on the leading edge of the point.

According to our numerical tsunami modelling, waves generated by a mega-thrust earthquake along the CSZ will be quite strong in Victoria Outer Harbour, reaching 1.7 to 2.3 m in the vicinity of the Coast Guard Base. In addition to the high wave amplitudes (up to 2.26 m for Model B), tsunamis will induce strong currents, up to 1.76 m/s in the area adjacent to the Coast Guard Base. Currents will be even stronger in the centre of the harbour.

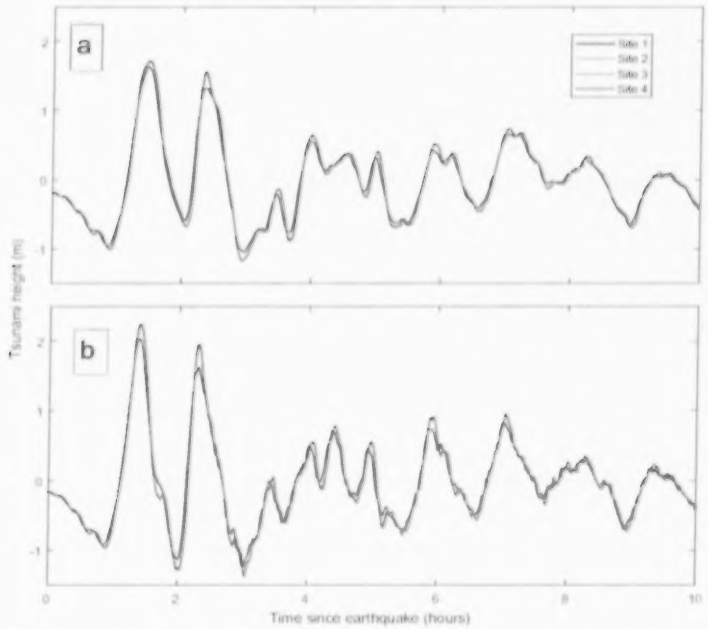

Figure 3.6. Simulated records of water level variations for a CSZ tsunami at Victoria Sites 1, 2, 3 and 4 (See Figure 3.5 for the site locations) for (a) Model A; and (b) Model B.

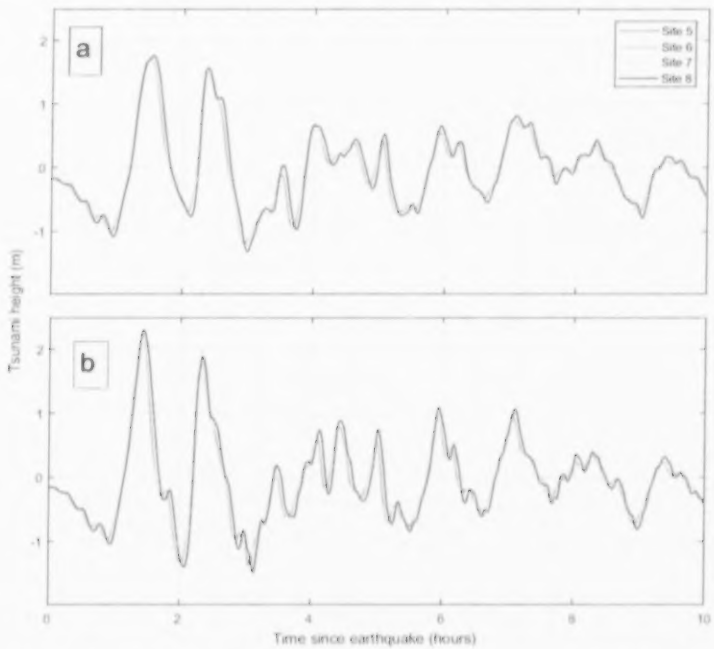

Figure 3.7. Simulated records of water level variations for a CSZ tsunami at Victoria Sites 5, 6, 7 and 8 (See Figure 3.5 for the site locations) for (a) Model A; and (b) Model B.

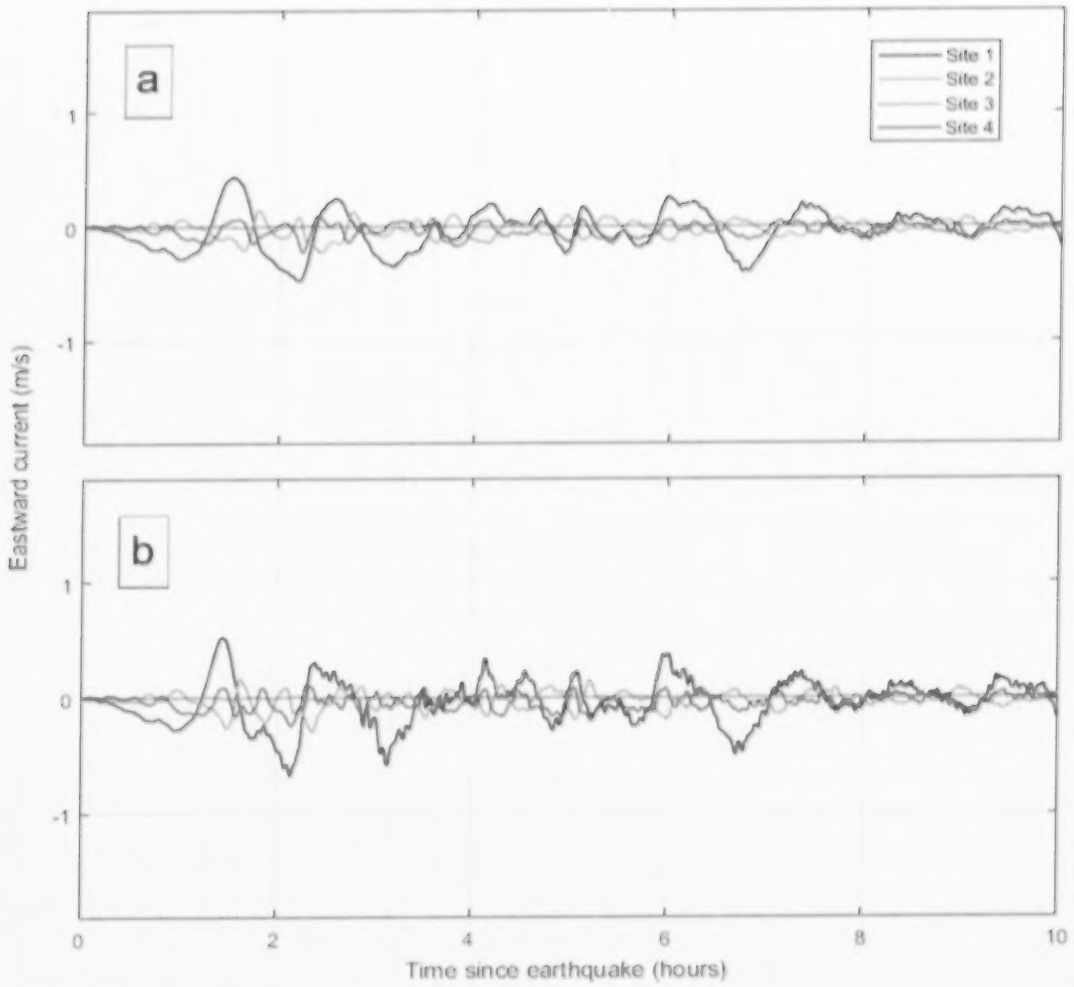

Figure 3.8. Simulated records of the eastward component of current velocity for a CSZ tsunami at Victoria Sites 1, 2, 3 and 4 (See Figure 3.5 for the site locations) for (a) Model A; and (b) Model B.

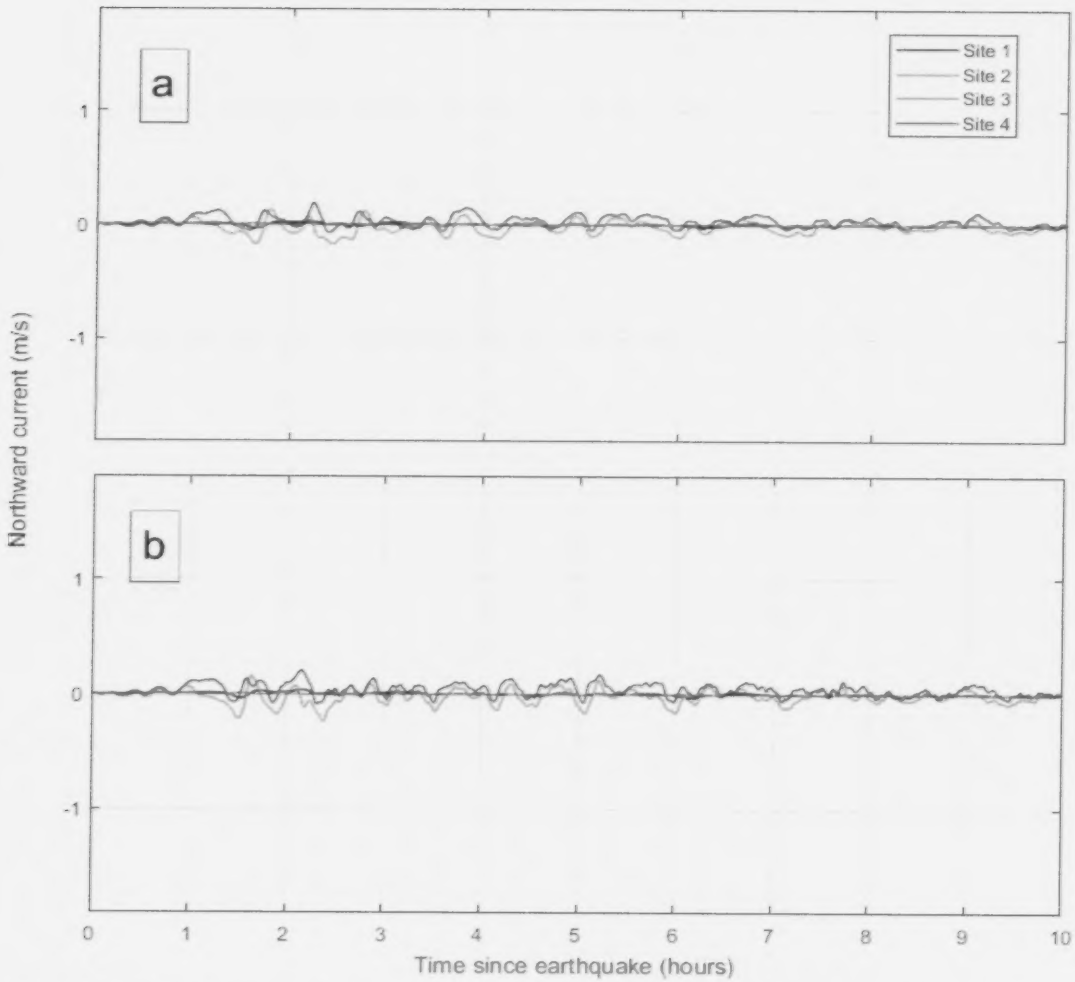

Figure 3.9. Simulated records of the northward component of current velocity for a CSZ tsunami at Victoria Sites 1, 2, 3 and 4 (See Figure 3.5 for the site locations) for (a) Model A; and (b) Model B.

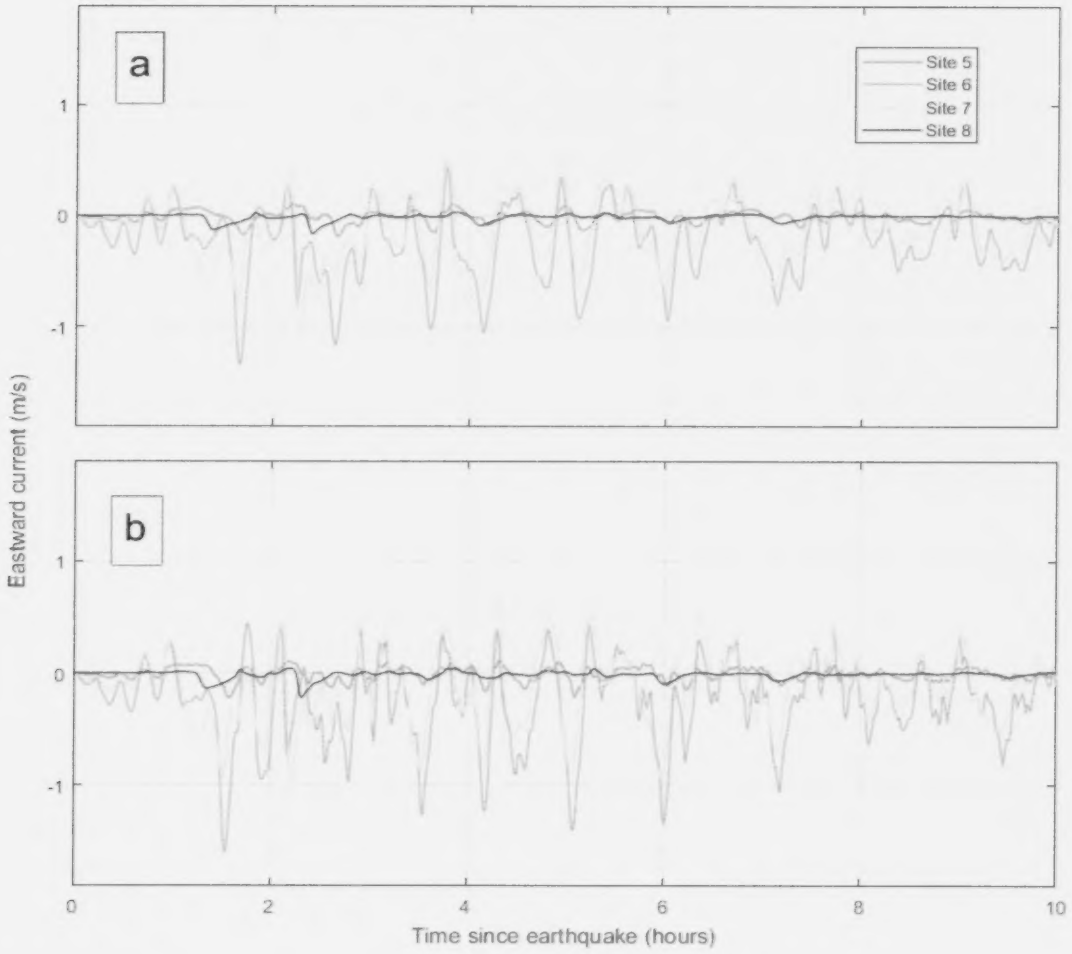

Figure 3.10. Simulated records of the eastward component of current velocity for a CSZ tsunami at Victoria Sites 5, 6, 7 and 8 (See Figure 3.5 for the site locations) for (a) Model A; and (b) Model B.

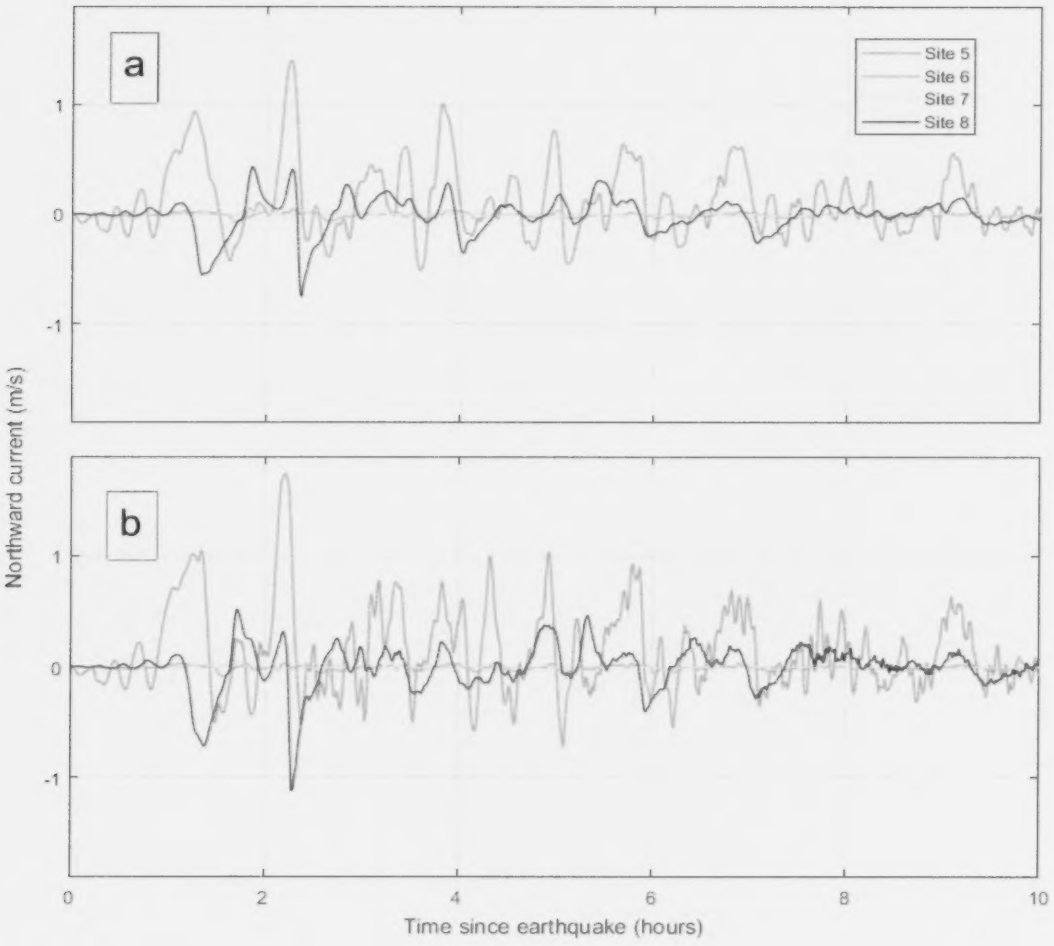

Figure 3.11. Simulated records of the northward component of current velocity for a CSZ tsunami at Victoria Sites 5, 6, 7 and 8 (See Figure 3.5 for the site locations) for (a) Model A; and (b) Model B.

This page is left intentionally blank

4 CONCLUSIONS

A high-resolution nested-grid tsunami model was used to simulate tsunami waves and wave-induced currents that will be generated in Victoria by a Cascadia Subduction Zone (CSZ) earthquake event. Two models of the earthquake rupture type and tsunami source region were used: Model A, a whole margin buried rupture; and Model B, a whole margin splay-faulting rupture. As recommended by international protocol, the numerical tsunami simulations were based on water depths above Mean Higher High Water (MHHW). For the Victoria tide gauge site, MHHW is 0.73 m above Mean Sea Level (MSL). The major results of the numerical modelling for the Victoria area are as follows:

- The whole margin splay-faulting rupture scenario (Model B) generates higher waves in the Victoria area than the whole margin buried rupture scenario (Model A). Model B can be considered as "worst case scenario" for the area;
- The maximum wave heights at the Coast Guard base will be 1.72 m (Model A case) and 2.26 m (Model B case) above the tidal level at the time of the event; the first-crest wave will be the highest wave; the maximum tsunami wave heights will occur from 1h 25 min to 1 h 30 min after the start of the earthquake;
- Model B (the worst case earthquake), together with the MHHW adjustment and the fact that a CSZ earthquake will cause the land in the Victoria region to suddenly subside by about 20 cm, will cause tsunami waves at the Victoria Coast Guard base to reach a net maximum height of:
    - 0.2 m + 2.26 m + 0.73 m = 3.19 m above MSL;
- Tsunami wave periods will range from 25 to 70 minutes;
- Tsunami wave amplitudes will be nearly spatially uniform throughout the Coast Guard base location;
- Sea level will drop about 20 cm immediately after the start of the earthquake due to land subsidence and the leading tsunami wave (a wave trough) will cause the water level to temporarily fall an additional 1 m below tidal level as it passes;
- Tsunami-induced currents in the vicinity of the Coast Guard base will be weak in the cove areas (Sites 2 to 4) and strong around the headlands (Sites 5 to 7); the strongest currents are 1.4 m/s (Model A) and 1.76 m/s (Model B);

Because many of the details of future possible tsunamis remain unknown, including the tidal level at the time of the event, uncertainties in the earthquake source distribution, possible storm surge or other oceanic events, we recommend that a safety factor of 50 % be added. This gives an estimated sea level height of 4.79 m above MSL (=1.5 × (2.26 m + 0.73 m + 0.2 m)) for a Model B-type CSZ tsunami.

More detailed predictions on the landward extent of tsunami wave run-up and inundation in the Victoria region will require more advanced numerical simulations, which permit wetting and drying of the land. The model should be able work with strong nonlinearity and friction, and incorporate discontinuity between wet and dry domains. Such studies also require detailed coastal elevation data and Lidar bathymetry along the shoreline. Future model upgrades should also take into account new advances in CSZ earthquake source regions developed by geophysicists.

5 ACKNOWLEDGEMENTS

The authors gratefully thank Peter Wills and Denny Sinnott of the Canadian Hydrographic Service for providing the bathymetric data and tide gauge records for this study, Alexander Rabinovich and Maxim Krassovski of the Institute of Oceanographic Science, for assisting with the data processing and numerical grid formulation, and Kelin Wang of Geological Survey of Canada, Natural Resources Canada for providing us his latest source models for the Cascadia earthquake and tsunami. We also thank Alison Scoon for helping transform the original report into a formal technical report.

This page is left intentionally blank

6 REFERENCES

AECOM (2013). Modelling of Potential Tsunami Inundation Limits and Run-Up, Capital Regional District, Project No. 6024 2933, 36 p.

Atwater, B.F. et al. (1995), Summary of coastal geologic evidence for past great earthquakes at the Cascadia Subduction Zone, Earthquake Spectra, 11 (1), 1-18.

Becker, J. J., D. T. Sandwell, W. H. F. Smith, J. Braud, B. Binder, J. Depner, D. Fabre, J. Factor, S. Ingalls, S-H. Kim, R. Ladner, K. Marks, S. Nelson, A. Pharaoh, R. Trimmer, J. Von Rosenberg, G. Wallace, P. Weatherall (2009). Global Bathymetry and Elevation Data at 30 Arc Seconds Resolution: SRTM30_PLUS, Marine Geodesy, 32:4, 355-371, DOI: 10.1080/01490410903297766.

British Columbia 3 arc-second Bathymetric Digital Elevation Model (2017). https://www.ngdc.noaa.gov/metaview/page?xml=NOAA/NESDIS/NGDC/MGG/DEM/iso/xml/4956.xml&view=getDataView&header=none.

Cherniawsky, J.Y., Titov, V.V., Wang, K., and Li, J.Y. (2007), Numerical simulations of tsunami waves and currents for southern Vancouver Island from a Cascadia megathrust earthquake, Pure Appl. Geophys. 164 (2-3), 465-492, DOI: 10.1007/s00024-006-0169-0.

Cheung, K.F., Wei, Y., Yamazaki, Y., and Yim, S.C.S. (2011), Modeling of 500-year tsunamis for probabilistic design of coastal infrastructure in the Pacific Northwest, Coastal Engineering 58 (2011) 970–985.

Clague, J.J., Bobrowsky, P.T., and Hutchinson, I. (2000), A review of geological records of large tsunamis at Vancouver Island, British Columbia, and implications for hazard, Quatern. Science Rev., 19, 849-863.

Clague, J.J., Munro, A., and Murty, T.S. (2003), Tsunami hazard and risk in Canada, Natural Hazards 28 (2-3), 433-461.

Dragert, H., and Rogers, G.C. (1988), Could a megathrust earthquake strike southern British Columbia? GEOS, 17 (3), 5-8.

Fine, I.V., Cherniawsky, J.Y., Rabinovich, A.B., and Stephenson, F.E. (2008), Numerical modeling and observations of tsunami waves in Alberni Inlet and Barkley Sound, British Columbia, Pure Appl. Geophys. 2008, 165, (11/12), 2019-2044.

Gao, D. (2016). Defining Megathrust Tsunami Sources at Northernmost Cascadia Using Thermal and Structural Information. Master of Science Thesis, School of Earth and Ocean Sciences, The University of Victoria, https://dspace.library.uvic.ca/handle/1828/7435.

GEBCO (The General Bathymetric Chart of the Oceans). http://www.gebco.net/. Last access on November 20, 2016.

Leonard, L.J., Rogers, G.C. and Mazzotti, S. (2014). Tsunami hazard assessment of Canada, Natural Hazards, 70, 237-274.

Myers, E.P., Baptista, A.M., and Priest, G.R. (1999), Finite element modelling of potential Cascadia subduction zone tsunamis, Sci. Tsunami Hazards, 17, 3–18.

Ng, M.K.-F., LeBlond, P.H., and Murty, T.S. (1990), Numerical simulation of tsunami amplitudes on the coast of British Columbia due to local earthquakes, Sci. Tsunami Hazards 8, 97-127.

Ng, M.K.-F., LeBlond, P.H., and Murty, T.S. (1991), Simulation of tsunamis from great earthquakes on the Cascadia subduction zone, Science 250, 1248–1251.

Satake, K., Shimazaki, K., Tsuji, K., and Ueda, K. (1996), Time and size of a giant earthquake in Cascadia earthquake inferred from Japanese tsunami records of January 1700, Nature 379, 246–249.

Thomson, R. E. and Emery, W. J. (2014). Data Analysis Methods in Physical Oceanography: 3rd Edition. Elsevier Science, Amsterdam, London, New York (August 2014), 716 p.

Wang, X. (2009). User Manual for COMCOT Version 1.7: http://ceeserver.cee.cornell.edu/pll-group/doc/COMCOT_User_Manual_v1_7.pdf.

Wang, K., and Tréhu, A.M. (2016), Invited review paper: Some outstanding issues in the study of great megathrust earthquakes—The Cascadia example, J. Geodynamics, 98, 1-18.

Whitmore, P.M. (1993), Expected tsunami amplitudes and currents along the North American coast for Cascadia Subduction Zone earthquakes, Natural Hazards 8, 59–73.

Witter, R.C., Zhang, Y.J., Wang, K., Priest, G.R., Goldfinger, C., Stimely, L., English, J.T., and Ferro, P.A. (2013). Simulated tsunami inundation for a range of Cascadia megathrust earthquake scenarios at Bandon, Oregon, USA, Geosphere, 9 (6), 1783-1803, DOI: 10.1130/GES00899.1.